



## Assessing the influence of climate change on sediment dynamics in the proposed makhool dam reservoir, Iraq



Nisreen J. Rasheed <sup>a,b\*</sup>, Mahmoud S. Al-Khafaji <sup>c</sup>, Imzahim A. Alwan <sup>a</sup>

<sup>a</sup> Civil Engineering Dept., University of Technology-Iraq, Alsina'a street, 10066 Baghdad, Iraq.

<sup>b</sup> Civil Engineering Dept., University of Diyala, Baqubah 32001, Diyala, Iraq.

<sup>c</sup> Water Resources Engineering Dept., University of Baghdad, Baghdad 10071, Iraq.

\*Corresponding author Email: [nisreen.j.r.h@uodiyala.edu.iq](mailto:nisreen.j.r.h@uodiyala.edu.iq)

### HIGHLIGHTS

- The impact of climate change on sediment transport in the Tigris River and its tributaries
- Assessment on how sediment transport affects the design life of the makhool dam reservoir
- The influence of the makhool dam reservoir on river flows is investigated
- The research formulates adaptive strategies and implements measures to mitigate the consequences of climate change

### ABSTRACT

Makhool Dam is a proposed structure on the Tigris River in the Salah al-Din Governorate, northwest of Baiji. The reservoir's sediment sources encompass the Tigris River, the Greater Zab River, and the Lesser Zab River. Climate change exerts a significant influence on both sediment accumulation within the dam reservoir and associated water resources. This paper specifically investigates the impact of climate change on sediment dynamics within the Makhool Dam reservoir. HEC-RAS 6.3.1 has been used to simulate the sediment dynamics and flow for the three rivers entering the reservoir. The SSP2-4.5 and SSP5-8.5 emission scenarios were applied to the 2021-2040, 2041-2060, 2061-2080, and 2081-2100 of 2021–2100. The calibration process of the model was performed using recorded water surface elevation measurements. The model was validated using the sediment concentrations at the proposed Makhool Dam. The sediment mass decreases along the rivers from upstream to downstream. The sediment mass is anticipated to decrease by approximately 20% and 35% from 2021 to 2100 under the SSP2-4.5 and SSP5-8.5 scenarios, respectively. For the studied future period, the estimated annual sediment deposition under the SSP2-4.5 and SSP5-8.5 scenarios is around 22×10<sup>6</sup> tons and 19×10<sup>6</sup> tons, respectively. In addition, under these scenarios, the potential life of the Makhool Reservoir is expected to be 95.7 and 109.5 years, respectively. The findings of this paper can play a vital role in supporting planners and decision-makers in performing efficient strategies for climate change adaptation and mitigating the impact of climate change.

### ARTICLE INFO

**Handling editor:** Mohammed A. Al-Neami

#### Keywords:

Climate change  
Tigris River  
Hydrodynamic  
Sediment transport  
Makhool Dam

## 1. Introduction

The Tigris River, which mainly stems from the southern region of Turkey, is the greatest in Western Asia [1]. It has a catchment area of 473103 km<sup>2</sup>, extended primarily in Turkey and less in Syria and Iraq [2]. The morphological aspects of river basins, such as topography, soil type, plan form, land use, and land cover, seriously affect the transported sediment load into and through the river. The intensity of yielded stream flow and sediment from the catchment areas into the tributaries and then to the main river significantly impacts the concentration and rates of transported sediment. During the rainy storms, in the wet season, the intensity, rate, and energy of flow increases; consequently, more potential sediment transport is gained. Therefore, excessive sediment is transported through the tributaries and main rivers to the downstream dam reservoirs. Sediment transportation through catchment discharge is significantly enhanced by precipitation, particularly during the start of the rainy season. Floods increase the stream flow velocity during this period, which causes a more significant number of particles to detach from the riverbed. This phenomenon enhances the stream's capability and efficacy. The flow velocity and energy are reduced when the river enters the reservoir, leading to sediment accumulation. Coarser sediment often settles toward the reservoir's inlet, while smaller particles settle toward the water flow within the reservoir [3].

Climate change will significantly affect water resources and the water cycle in the future [4]. Minor changes in rainfall patterns result in substantial changes in the streamflow, altering both the streamflow regime and associated processes [5]. Streamflow variations and fluvial processes greatly affect the amount of sediment carried by rivers [6]. Climate change indirectly led to morphological changes in rivers and reservoirs [7]. Streamflow changes cause flow velocity variations, bed erosion, and deposition, disturbing the sediment balance. Thus, it becomes evident that climate change can potentially modify hydrology and the hydraulic regime, ultimately leading to changes in river and reservoir morphology [8].

Makhool Dam is a major hydraulic project on the Tigris River in the northeastern region of Salah al-Din Governorate, approximately 30 km northeast of Baiji [9]. The expected consequences of climate change relate to water scarcity, high temperatures, and sudden flood waves in the Tigris River Basin. These changes substantially impact the river's morphology, leading to changes in the sediment deposition process and various aspects of the river flow [10]. As mentioned previously, the problem that needs to be considered regarding dams is the accumulation of sediments. This phenomenon engenders an augmented risk of flooding, attributable to a diminished capacity of the dam to retain water, subsequently compromising its efficacy in floodwater management. The reduced storage capability adversely affects the reservoir's capacity to meet diverse water requirements while concurrently upholding safety standards. In addition, the sediment deposition near the intake of the powerhouse and bottom outlet exerts a deleterious influence on the dam's operational performance.

Mathematical models are constructed using suitable numerical methods and logical reasoning, effectively and precisely simulating diverse scenarios. Alteration in river channels and flood plains can be efficiently assessed by using mathematical simulation models. The findings of such models support achieving accurate plans and making the right decisions toward sustainable strategies for the development of water resources [11]. In several studies, the HEC-RAS software was utilized to simulate sediment transport and compute river beds and reservoir changes [12] assessed the performance of the HEC-RAS software in computing the bed change in the Karun River. This assessment was based on a comparative analysis of the HEC-RAS with other software. This assessment showed that the HEC-RAS performs well in calculating hydraulic, sediment transport, and bed change details in rivers. Also, the HEC-RAS was used by Singley [13] to compute the concentration and rate of the transported sediment into the reservoir of Aguacate Dam in the Dominican Republic. The findings of this application provided vital sediment-related information. This information offers valuable insights for future dam design considerations. Amini et al. [14] simulate the sediment transport and flush out the sediment load from the Peru Dam reservoir to investigate the sediment distribution and determine the best management of reservoir sedimentation. To this end, an HEC-RAS-based one-dimensional model was implemented to determine the distribution of the bed and suspended load in the reservoir. Moreover, the HEC-RAS software was used by Mohammad et al. [3] to implement hydrodynamic and sediment transport dynamic models to investigate the flow and sediment transport aspects in the Tigris River and Mosul Dam reservoir in Iraq. Namaa et al. [15] used the same software to determine the hydraulic characteristics and sediment transport capacity of the Makhool-Samarra Reach of the Tigris River, Iraq.

Although several scholars used HEC-RAS-based simulation models to investigate the hydrodynamic and sediment transport aspects in dam reservoirs, the influence of climate change on these reservoirs was not the main focus of each of these investigations. Furthermore, the influence of sediment dynamics and accumulation caused by climate change in the Makhool Dam reservoir was not verified. This paper examines the impact of climate change by using two emission scenarios (SSP2-4.5 and SSP5-8.5) on the sediment dynamics in the reservoir of the proposed Makhool Dam by using the HEC-RAS 6.3.1 software. Understanding the changes in sediment due to climate change is imperative for basin planners and policymakers to adopt effective and sustainable mitigation and adaptation measures.

## 2. Material and methods

### 2.1 Makhool dam

The Makhool Dam is a significant and expansive project slated for construction on the Tigris River in Iraq. It is Situated in Salah Al-Din Governorate, northwest of Baiji, at 230 km to the north of Baghdad; it is positioned approximately 5 km downstream from the confluence of the Lesser Zab River with the Tigris River [9]. Astronomically, its location spans from 34° to 36° North latitudes and 38° to 39° longitudes (Figure 1). Makhool Dam was proposed for flood control and protection of the areas downstream of the dam, irrigation and agriculture, and electric power generation. After the operation, this dam will be considered among the largest dams in Iraq in the Tigris River basin. The total water storage capacity of the Makhool Dam reservoir is 2.9 km<sup>3</sup> at a maximum operation level of 150 m a.s.l. of which 1.914 and 0.986 km<sup>3</sup> are active and dead storages, respectively. A downstream spillway consists of 16 holes in the bottom, each with a width of 8 m and a height of 10 m. These holes are equipped with radial iron gates operated by a hydraulic system to control water discharge. The level of the bottom outlet holes is 120 m a.s.l. The total discharge capacity of the bottom outlet is 22225 m<sup>3</sup>/s when the reservoir level is 152.15 m above sea level. The emergency spillway is above the downstream spillway, rising beyond the maximum operating level of 150 m above sea level. The total discharge capacity of the spillway is 1338 m<sup>3</sup>/s at a level of 152.15 m a.s.l. This spillway also serves as a safety valve during high flood events. The sill of this spillway runoff is positioned at 150.25 m a.s.l. and takes the form of a curved weir of the Ogee type, channeling water into the same stilling basin as the downstream spillway. The dam will protect Baghdad City from flood danger and provide irrigation advantages. Therefore, the Makhool Dam project can be considered an essential strategic project in Iraq [16]. Sediment deposition poses a significant challenge for reservoirs; the Makhool Dam is also affected by the accumulation of sediment, especially in the top section of the reservoir. The primary sediment source to the reservoir is from Tigris River inflows, Greater Zab River inflow, and Lesser Zab River inflow.

The elevation-area-volume curve of a dam reservoir plays a significant role in estimating the most appropriate depth, highest capacity, and optimum surface area of a dam reservoir. Figure 2 illustrates the elevation-area-volume curve for the Makhool Reservoir. The significance of the reservoir's elevation-area-volume curve lies in anticipating the geometric features of the dam reservoir prior to construction. This curve facilitates the establishment of a database, enabling predictions about the reservoir's behavior during operation. Designers can depend on this information when creating plans for the dam structure.

The incoming water discharges of the Makhool Dam reservoir are notably influenced by the water releases from the Mosul and Dokan dams, alongside the inflow from the Greater Zab River. The operational commencement of the Dokan dam in 1960 and the Mosul dam in 1986 have significantly impacted the water discharges in this region, directly influenced by the outflows from these dams. Analyzing available data spanning the period from 1932 to 1999, it is observed that the highest average monthly discharge reached 6990 m<sup>3</sup>/s in April 1988, while the lowest monthly average discharge, recorded in September 1951, stood at 208 m<sup>3</sup>/s [16]. Unfortunately, due to the absence of data for the area from 2000 to 2020, information from the Baiji station was utilized. In April 2020, the highest average monthly discharge, totaling 8947 m<sup>3</sup>/s, was documented. This coincided with water discharges from the Dokan and Mosul dams and relatively high average rainfall within the river's feeding basin. The rating curve at the location of the proposed Makhool Dam is shown in Figure 3.

The Tigris River, from Mosul Dam to the location of Makhool Dam, flows on an undulating plain. The floodplain of the Tigris River consists mainly of silt, clay, rare sand, and pebbles. The pebbles are composed chiefly of silicates and carbonates, with a lesser presence of igneous and metamorphic rocks [17]. The predominant constituent of bed material in the Tigris River within Mosul and Tikrit is medium gravel [15]. The concentration of suspended sediment at the location of the proposed Makhool Dam is shown in Table 1. The Greater Zab in Iraq travels over rugged, mountainous terrain, flowing across undulating plains. The Lesser Zab flows through hilly regions, flat terrain, and gently undulating plains in its lower portions, while the higher parts flow through mountainous areas [10].

The Mosul-Makhool Basin (MMB) climate typically spans from semi-arid to arid regions. Semi-arid regions, in particular, are highly vulnerable to the impacts of climate change, resulting in a reduction in available water resources. In winter, air temperatures vary from below freezing (0°C) to over 18°C, depending on the season and location, while in summer, temperatures often exceed 45°C. Precipitation is most common between October and April, with snowfall being most frequent from January to March. The average annual precipitation amounts vary between 180 and 1500 mm [18].

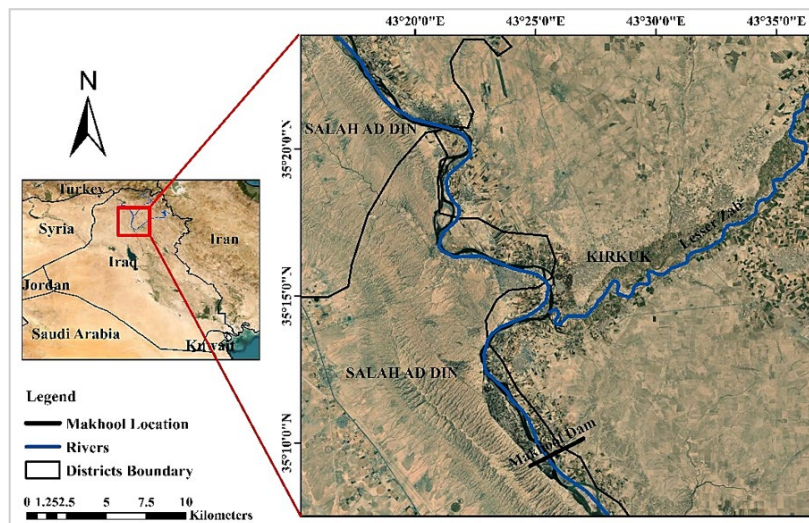


Figure 1: The location of makhool dam

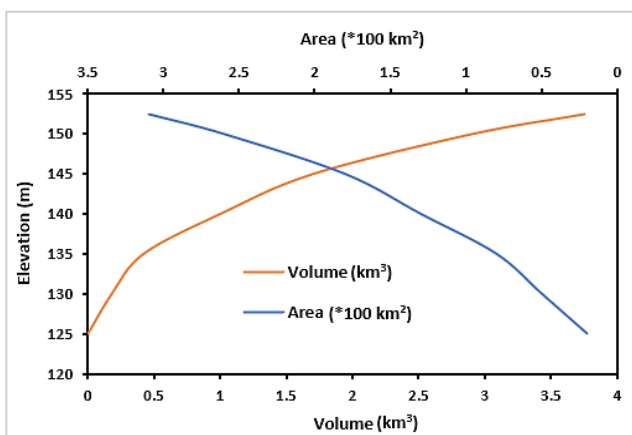


Figure 2: Elevation-area- volume curve for makhool reservoir [16]

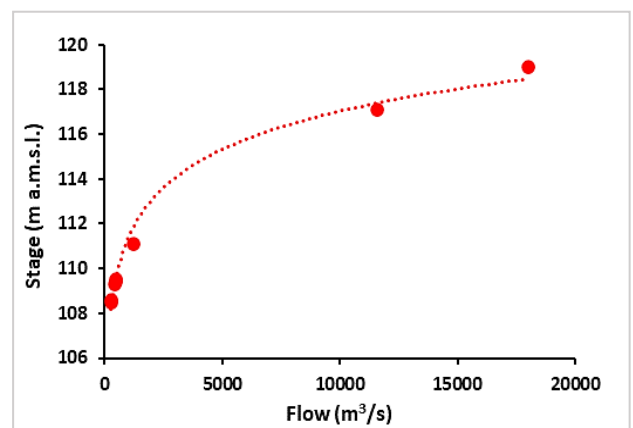


Figure 3: The rating curve at the location of the proposed makhool dam

**Table 1:** Concentration of suspended sediment at the location of makhool dam [15]

Date	Concentration of sediment (mg/l)
9-Sep-21	31.3
21-Oct-21	17.9
18-Nov-21	75.6
29-Dec-21	151.9
27-Jan-22	251.7
24-Feb-22	349.0
10-Jun-22	69.5

## 2.2 Hydrological computations and climate change scenarios

The impact of climate change on the reservoir of the proposed Makhool Dam was evaluated using the findings presented in the study by Rasheed et al., (2024) [19] used the Soil and Water Assessment Tools (SWAT) Model to examine the impact of climate change on the hydrological characteristics of the MMB. The dataset from the Coupled Model Intercomparison Project Phase 6 (CMIP6) was used to evaluate projected future changes in temperature and precipitation for the period spanning from 2021 to 2100 [19].

Rasheed et al., [19] conducted a simulation to model the hydrological response of the MMB under various climatic scenarios. They examined two emission scenarios: SSP2-4.5 (medium emission) and SSP5-8.5 (high emission). The study separated the period into four time intervals: 2021–2040, 2041–2060, 2061–2080, and 2081–2100. These scenarios were employed to calculate sediment yield and streamflow within the studied basin. The SWAT model produced streamflow and sediment yield results, essential boundary conditions for the subsequent Hydrologic Engineering Center-River Analysis System (HEC-RAS) modeling phase.

## 2.3 Hydrodynamic model

HEC-RAS software, utilized in this study, primarily works with the Saint-Venant equations, a set of partial differential equations that describe the one-dimensional flow of shallow water in open channels. These equations are often used in hydraulic simulation models of open-channel river flow. HEC-RAS software solves these sets of equations to simulate the flow in rivers and channels and to determine the flow characteristics such as water surface elevation, water depth, flow velocities, shear stress, etc. By incorporating the principles of mass and momentum conservation, the Saint-Venant equations provide a robust theoretical framework for modeling the dynamic behavior of river systems.

The input data required are the flow rate, topography, and roughness coefficient to simulate the flow using the hydrodynamic model. The upstream boundary condition is the flow rate from Greater Zab and the outflow from Mosul Dam and Dokan Dam, while the rating curve at the location of Makhool Dam is the downstream boundary condition (Figure 3). The upstream flow data and downstream flow data were taken from the results of the SWAT model. The channel geometry data was created from the Digital Elevation Model (DEM) to establish the topography of the study area in 3D. The DEM with a resolution of 12.5 m × 12.5 m was obtained from ALOS PALSAR; the dataset provider is JAXA Earth Observation Research Center, available at (<http://https://search.asf.alaska.edu/#/>).

The river centerline was established through the digitization process of the Greater Zab River and the Lesser Zab River, extending from Dokan Dam (upstream) to its confluence with the Tigris River (downstream). Simultaneously, the Tigris River was digitized from the Mosul Dam (upstream) to the anticipated location of the Makhool Dam (downstream). After this, the riverbanks and flow paths for the right bank of both rivers were digitized initially, followed by the left bank, proceeding from upstream to downstream. Concurrently, relevant attribute information was assigned to these digitized features. Elevation data was extracted from the DEM by generating cross-sectional lines representing terrain characteristics. These cross-sectional lines intersected with the river's central axis and flow routes, yielding crucial data points. This dataset encompassed downstream segment lengths, the positioning of riverbank stations, and Manning values. Spaced at approximately 500 m intervals, perpendicular cross-sectional lines were delineated concerning the river's central axis, extending from left to right when viewed downstream. The integration of attribute information, such as reach lengths, river profiles, bank station positions, and elevations, was undertaken within the RAS Mapper tool to enhance the functionality and comprehensiveness of these cross-sectional lines.

The model incorporates Manning's roughness coefficient ( $n$ ) value, representing the resistance to flow within rivers' main channels and floodplains regarding the bed roughness and land cover. The river profiles are allocated the Manning roughness coefficients ' $n$ '. Each cross-sectional line required three ' $n$ ' values: one for the main channel and two for the floodplain. Due to the scarcity of data necessary to identify the primary values of Manning's ' $n$ ' for river overbanks, this study has assigned ' $n$ ' values to overbank regions based on the study by Arcement and Schneider [20]. This approach, as developed by Emery et al. [21], employed satellite imagery, land use/land cover (LULC), and sediment data. The satellite images for the study area are available from the United States Geological Survey (USGS) with a spatial resolution of 30 m, accessible at the following website: <https://earthexplorer.usgs.gov/>. The LULC data were sourced from ESRI, providing a spatial resolution of 10 m, available at <https://livingatlas.arcgis.com/landcover/>. Global soil data was also derived from the Food and Agriculture Organization of the United Nations (1995). The ' $n$ ' values for the main channel were obtained through model calibration. A set of measured water surface elevation and/or velocity values is required for the calibration process. However, essential statistical indicators are utilized to evaluate the model's performance. The Nash-Sutcliffe efficiency (NSE), coefficient of determination

( $R^2$ ), and Ratio of Standard Deviation of Errors to Observations (RSR) are commonly employed statistical metrics for assessing the level of agreement between observed and computed hydraulic parameters during the calibration and validation stages.  $NSE > 0.5$ ,  $R^2 > 0.6$ , and  $RSR < 0.7$  are satisfactory [22].

Setting boundary conditions is vital in establishing the initial water depth at downstream and upstream locations. These conditions are fundamental in determining the initial water surface levels at both ends of the simulated river system [23]. To determine a supercritical flow regime, it's essential to focus on boundary conditions exclusively at the upstream ends of the river system, and the calculation begins from the upstream and moves downstream. In the case of a subcritical flow regime, it's imperative to specify boundary conditions solely at the downstream ends of the river system, and the computation starts in the downstream segment and proceeds upstream. When dealing with a mixed flow regime, both downstream and upstream boundary conditions must be provided at all open ends of the river system [24,25]. In this study, subcritical flow will be used. The HEC-RAS-based model comprises four classes of boundary conditions: known Water Surface Elevation (WSE), rating curve, normal depth, and critical depth. Suitable boundary conditions are specified based on the flow regime of the river under consideration. In this study, the rating curve is used as a boundary condition at the downstream end of the river.

## 2.4 Sediment transport model

Sediment transport is computed with the Exner equation; the Exner equation is considered to handle sediment routing and solve the sediment continuity equation, as shown in Equation (1):

$$(1 - \lambda_p) \frac{\partial el}{\partial t} = \frac{\partial Q_s}{\partial x} \quad (1)$$

where:  $B$  is the width of a channel;  $el$  is the bed elevation of a channel;  $\lambda_p$  is the porosity of the active layer;  $t$  is time;  $x$  is length; and  $Q_s$  is the sediment load.

The porosity of the active layer is essential for converting the mass change into volume. HEC-RAS employs the deviation between the inflow and outflow of sediment within the control volume (which corresponds to the right-hand side of Equation (1)) to compute the variation of bed thickness over time [26–31].

Determining the sediment outflow from the control volume is challenging due to the complicated connection between hydraulic factors and sediment properties. HEC-RAS simplifies this by computing the sediment transport capacity, representing the mass of sediment that can be transported for each specific grain size in the active layer. The deposition and erosion quantities are assessed separately for each grain size class by comparing the calculated sediment transport potential with the amount of inflow sediment from the upstream. If sediment inflow exceeds the transport capacity, the excess sediment is deposited. On the other hand, if sediment inflow is less than the transport capacity, the sediment deficit is eroded from the river bed, ensuring that the sediment continuity equation is satisfied [26]. In HEC-RAS, multiple sediment transport equations are available to calculate the sediment transport potential. However, these formulas are intended to handle specific ranges of particle sizes. Therefore, dealing with any of these formulas requires carefully considering the limitations of each formula and employing engineering expertise in choosing the appropriate formula.

A quasi-unsteady flow theory and boundary conditions, where the flow hydrograph is divided into a series of short intervals of steady flow, are usually used for modeling sediment transport in rivers. This method can compute the water depth, flow velocity, suspended and bed sediment load, and other hydrodynamic aspects at each interval according to the change in river geometry and boundary conditions. Furthermore, using this method to simulate the unsteady flow conditions in rivers with rapidly changing flow conditions, the HEC-RAS-based simulation model produces a comprehensive and precise characterization of the hydrodynamic and sediment transport behavior better than utilizing the purely steady flow.

To simulate the sediment transport, the input data required are the flow rate, sediment data topography, roughness coefficient, and grain size distribution data. The upstream boundary condition is the flow rate and sediment data from the Greater Zab River and the outflow and sediment from Mosul and Dokan Dam. At the same time, the rating curve at the location of Makhool Dam is the downstream boundary condition. The upstream and downstream data were taken from the results of the SWAT model.

## 3. Results and discussion

### 3.1 Calibration and validation of HEC-RAS-based model

The calibration process of the model was performed by using recorded measurements at 32 specific locations within the considered reach of the Tigris River to decrease uncertainty and enhance the model's robustness within the limitations of available data. Steady-state conditions in the hydrodynamic model have been used in the calibration process. The calibration process depended on matching the observed WSE of these locations with the simulated WSE to calibrate the roughness coefficient. Nevertheless, it's essential to know that if there had been a time series of observed sediment data within the model's area, calibrating the model with such data could have further minimized uncertainties in simulating bed-level changes. After several iterations, the calibration process revealed a significant agreement between the observed and computed WSE, with  $NSE$ ,  $R^2$ , and  $RSR$  of 0.85, 0.81, and 0.05, respectively. The  $n$  values for the main channel varied from 0.02 to 0.035, while they ranged from 0.03 to 0.051 for the floodplain. The evaluation of statistical parameters confirms that the model effectively simulates morphodynamic processes with satisfactory performance. Figure 4 illustrates the final comparison along the river between the observed and computed WSE.

The model validation process involved comparing the observed sediment concentration at the proposed Makhool Dam site, as shown in Table 1, with the corresponding simulated sediment concentration generated by the model. This validation procedure was instrumental in determining the most suitable equation for the simulation process. HEC-RAS offers eight different formulas for sediment transport calculations. Based on the validation outcomes, the Laursen-Copeland model has been selected for utilization in this study. This particular equation defines a total-load equation with a transport function applicable to a wide range, covering gravel and coarse silt. This characteristic endows it with the broadest range of applicability among the equations provided by HEC-RAS. The evaluation results demonstrated a satisfactory level of validity, with NSE,  $R^2$ , and RSR values of 0.62, 0.61, and 0.09, respectively, as depicted in Figure 5.

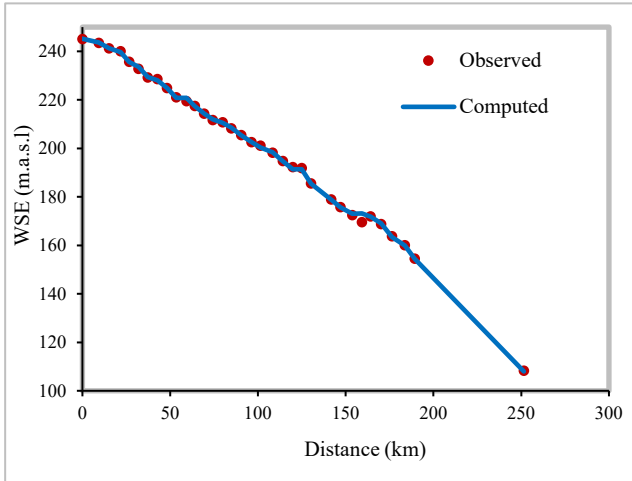


**Figure 4:** Compares the observed and computed WSE along the river

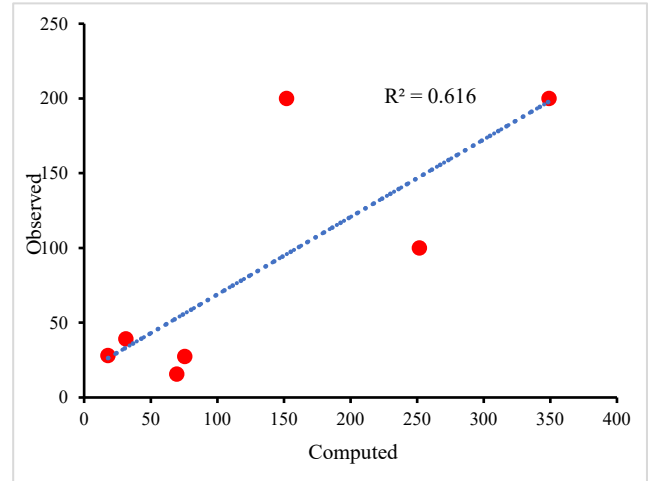


**Figure 5:** Comparison of observed and computed sediment concentrations at makhool dam for model validation

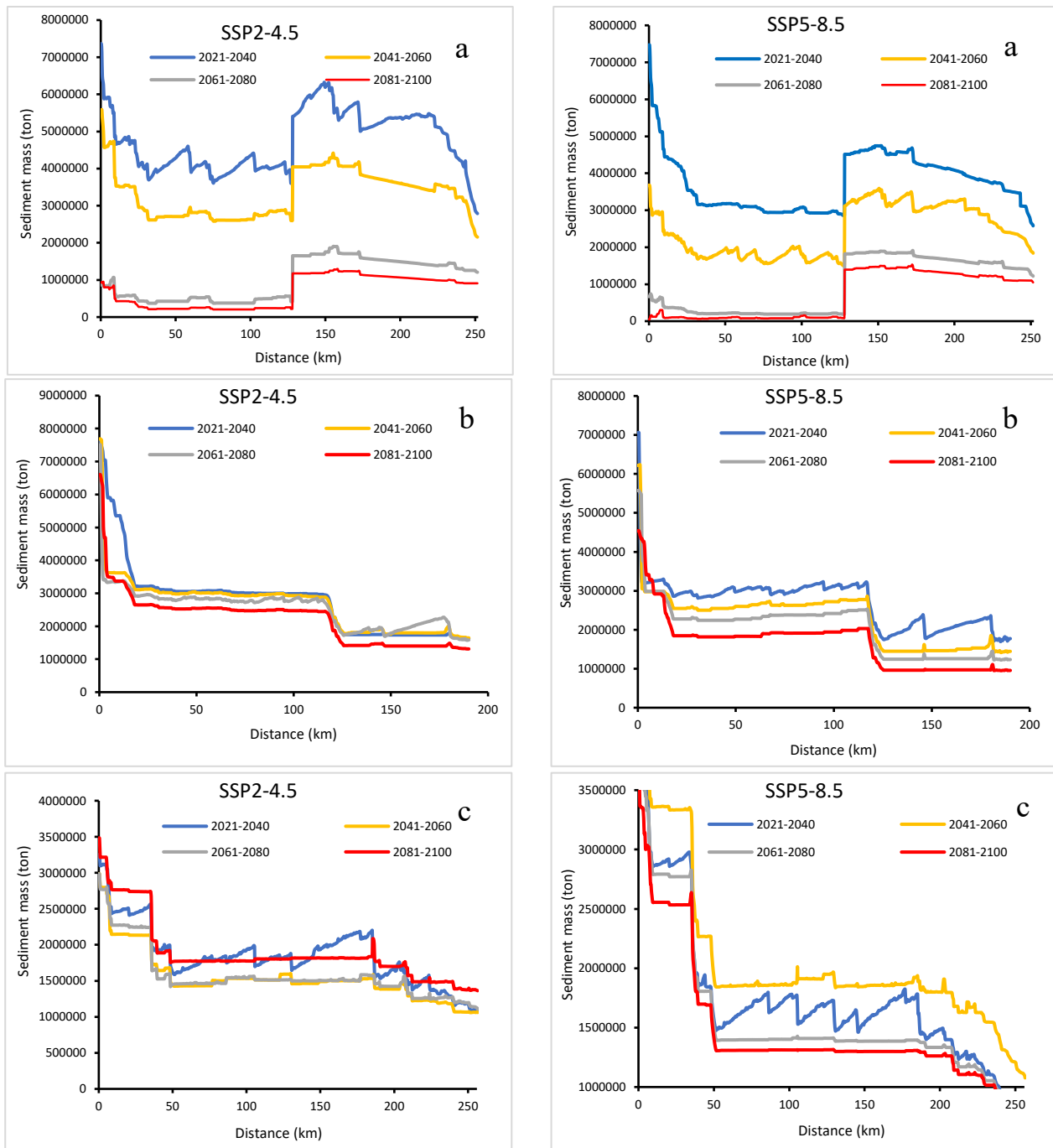
### 3.2 Spatial distribution of sediment mass along the river system under climate change scenarios

Figure 6 provides a graphical representation of the spatial distribution of sediment mass, measured in tons, across the three rivers (Tigris River, Greater Zab, and Lesser Zab). This illustration spans four future periods and encompasses two distinct emission scenarios, namely SSP2-4.5 and SSP5-8.5. This analysis aims to elucidate the influence of climate change on the sediment distribution along the considered rivers. Figure 6(a) depicts the spatial distribution of sediment mass along the Tigris River. Notably, a substantial increase in sediment mass is anticipated at a distance of 128 km, coinciding with the confluence of the Greater Zab with the Tigris River. Subsequently, the sediment mass stabilizes until reaching a distance of 173 km from the upstream, after which a gradual decrease is projected. This decline is attributed to the influence of the Makhool Dam reservoir extending to this distance.

From a climate change perspective, a temporal analysis indicates a consistent decrease in sediment mass as the timeline progresses, extending until 2100. This decrease is attributed to anticipated reductions in streamflow resulting from diminished precipitation and elevated temperatures in the future [19]. Notably, under the SSP5-8.5 scenario, the sediment mass exhibits a decline of 3.5 mg/l in comparison to the SSP2-4.5 scenario. The spatial distribution of sediment mass along the Greater Zab is depicted in Figure 6(b). An abrupt reduction in sediment mass is evident for all future periods, particularly at a distance of 70 km from the confluence of the Greater Zab with the Tigris River near Shaqlawa City.

Furthermore, a temporal analysis reveals a consistent decline in sediment mass over future periods. Specifically, the sediment mass is anticipated to decrease by approximately 20% from 2021 to 2100 under the SSP2-4.5 scenario. In the same context, the sediment mass is expected to reduce by about 35% until the end of the century under the SSP5-8.5 scenario. Global warming and changes in land use could be the reason for the observed decrease in sediment mass. The sediment mass dynamics along the Lesser Zab are shown in Figure 6(c). A significant decrease in sediment mass is observed at a distance of 50 km from Dokan Dam. After this point, the sediment mass stabilizes until it reaches a distance of 203 km, where it gradually decreases until the Lesser Zab River conflues the Tigris River. This decrease in sediment mass is attributed to the influence of the Makhool Dam, which extends to this distance. From a temporal perspective, the behavior of Figure 6(c) predicts a decrease in sediment mass over time until the end of the current century. In particular, for the scenario of SSP2-4.5, there is a decline in the deposited sediment mass by 16% at the end of 2021 to 2100. However, this decline is more evident in the scenario of SSP5-8.5, with a percentage of 18% for the same period.

This simulation contributes to an accurate assessment of the effects of climate change and its impact on the dynamics of sediment transport in rivers. This work represents a valuable tool for monitoring sediment mass distribution along rivers and explains the complex interactions between climate change and river morphology.



**Figure 6:** Expected impacts of climate change on sediment mass along river systems, (a) Tigris River, (b) Greater Zab, and (c) Lesser Zab

### 3.3 Impact of Makhool dam reservoir on Tigris river

The reservoir consists of two sections: the first segment stretches along the Lesser Zab River. In contrast, the second segment extends northward of the Tigris River, converging near the current mouth of the Lesser Zab River with the Tigris River. Notably, the longitudinal extension of the reservoir body is greater towards the Tigris River than towards the Lesser Zab River. This discrepancy can be attributed to the regional topography, where the slope is more pronounced in the Lesser Zab region than the Tigris River's primary course. The length of the reservoir in the north direction reaches 75 km, and an average width of 3.1 km parallel to the current course of the Tigris River when the reservoir level reaches 150 m a.s.l. At the same time, its length, in a direction parallel to the course of the Lesser Zab River, reaches 50 km, with an average width of 0.5 km at the same elevation. Figure 7 illustrates the reservoir of the Makhool Dam. When the flow enters the reservoir, the flow velocity and the power decrease, which causes sediment to deposit in the reservoir. The eroded material, called eroded soil, resulting from rain-induced torrents that complete their journey from the source, can enter the reservoir in suspended or bed load. These two components collectively constitute the total sediment load. Typically, a significant portion of the sediment load is suspended in most rivers, comprising approximately 80 to 90 percent of the total sediment load [3].

The deposition of sediment in the Makhool Dam Reservoir exhibited variation across various future periods, with the highest proportions (79.1 and 78) occurring during the initial 20 years (2021–2040) of dam operation under SSP2-4.5 and SSP5-8.5, respectively. The sedimentation rate gradually declined over time, a trend attributed to the decelerated flow rate of the Tigris River and its tributaries since the commencement of dam operation.

The anticipated percentages of the total sediment load entering the reservoir during the contemplated future periods (2040, 2060, 2080, and 2100) are projected to be 0.48, 0.31, 0.12, and 0.09 under the SSP2-4.5 scenario. Similarly, the corresponding percentages under the SSP5-8.5 scenario are expected to be 0.49, 0.34, 0.10, and 0.07 for the same future periods, as shown in Figure 8. The sedimentation rate gradually declined over time, a trend attributed to the elevated flow rate of the Tigris River and its tributaries since the commencement of dam operation. The reduction in sediment load in MMB under SSP5-8.5 scenarios is underscored by the study conducted by [19]. They anticipated a 55% decrease in sediment yield for SSP5-8.5 scenarios, in contrast to a 46% reduction in the case of SSP2-4.5 scenarios. The expected decline in sediment load over the forthcoming years can be attributed to a projected decrease in precipitation, estimated at 9.5% and 18.7% under SSP2-4.5 and SSP5-8.5 scenarios, respectively, by the conclusion of the 21st century.

Most sediment originating from the catchment area of the Tigris River and Lesser Zab River is retained by the Mosul Dam and Dokan Dam, respectively. However, sediments within the Makhool Reservoir will be sourced from small tributaries and the bottom erosion process. Notably, the Greater Zab River will contribute a significant portion of these sediments, as it lacks a substantial reservoir. Projections indicate that the mass of sediments in the Makhool Dam area is anticipated to amount to approximately 22 million tons annually under the SSP2-4.5 scenario. Conversely, under the SSP5-8.5 scenario, the expected annual sediment mass is projected to be around 19 million tons. These estimates provide insights into the potential sedimentation dynamics in the reservoir under different scenarios, emphasizing the importance of considering such variations in the dam's planning and management.

The Euphrates Center has estimated the permanently submerged density of a combination of equal proportions of clay, silt, and sand to be  $1,280 \text{ kg/m}^3$  and the sedimentation efficiency to be 60% [16]. Consequently, the computed annual volume occupied by sedimentation is  $10.3 \text{ million m}^3$  for SSP2-4.5 and  $9 \text{ million m}^3$  for SSP5-8.5, assuming the absence of the Bakhme Dam. Considering that the lowest operational level is set at 140 m a.s.l. and relying on the Hydrological Study of Makhool Dam [16] utilizing the elevation-area-volume curve of the Makhool Dam, the volume of the reservoir at this specified level is determined to be 986 million cubic meters.

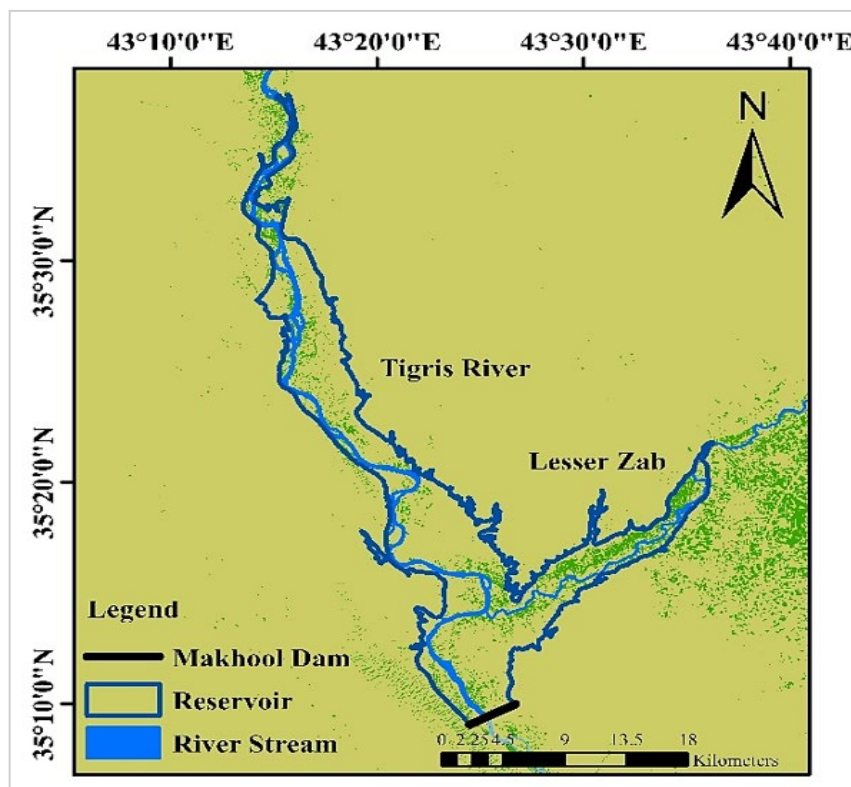
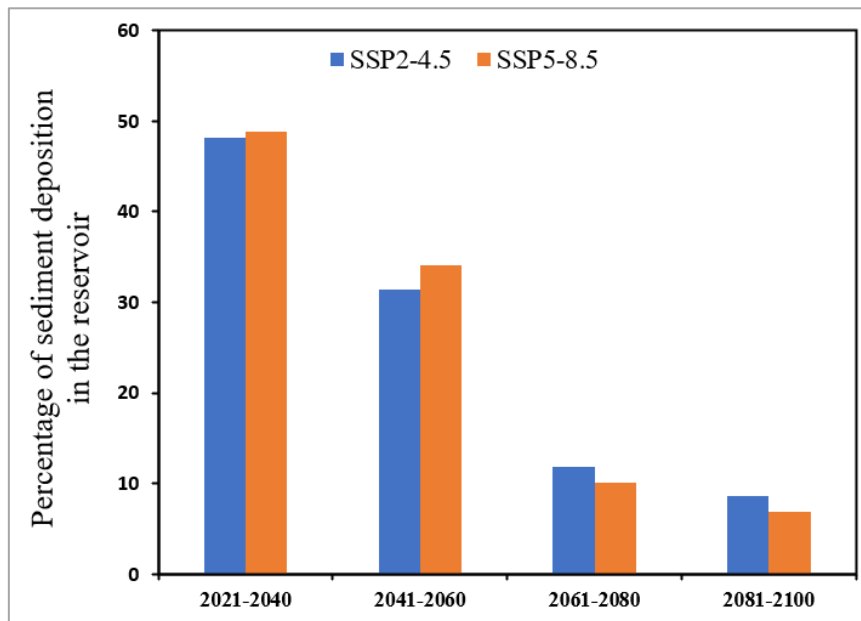


Figure 7: Reservoir location of Makhool Dam

This adjustment implies that the design life of the Makhool Reservoir would extend to 95.7 years under SSP2-4.5 and 109.5 years under SSP2-8.5. The hydrological study of Makhool Dam [16] provided additional sediment characteristics, indicating a specific weight ( $G_s$ ) of 2.65 and a sediment diameter ( $d_{50}$ ) of 12.4 mm. Considering a substantial flow through the lower outlet at a threshold of 120 m.a.s.l, the study anticipated that sedimentation is not expected to pose a problem in the Makhool Reservoir.





**Figure 8:** Variation in sediment deposition percentage within the makhool dam reservoir across various future periods

#### 4. Conclusion

The HEC-RAS model was employed to simulate flow and sediment routing within the proposed Makhool Dam reservoir to predict the impact of climate change on the said reservoir. The simulation spanned from 2021 to 2100, considering two emission scenarios (SSP2-4.5 and SSP5-8.5). Calibration and validation of the model were conducted for both flow and sediment aspects, utilizing available measured data. The results indicated a satisfactory performance for the model for flow simulation and sediment concentration. The sediment mass increases at the confluence of the Greater Zab tributary with the Tigris River. Moreover, the sediment mass is anticipated to decrease in the future, which is attributable to the impact of climate change. The projected reservoir dimensions indicate a span of approximately 75 km across the Tigris River and 50 km across the Lesser Zab River. The projected annual total sediment load deposition is expected to reach 22 million tons under the SSP2-4.5 scenario, with a concurrent reduction of 13% under the SSP5-8.5 scenario. Notably, a substantial proportion of these sediments (79.1%) will accumulate within 20 years of the dam's operation, underscoring its effective sediment-trapping capability during the early operational phases. The study's results suggest that the Makhool Reservoir's design life could extend to 95.7 years under SSP2-4.5 and 109.5 years under SSP5-8.5. Enhanced outcomes concerning sediment deposition in reservoirs could be achieved with improved data availability. The implications of this research offer valuable insights for informed decision-making, facilitating proactive measures, and enhancing preparedness to address the challenges posed by climate change.

#### Author contributions

Conceptualization, N. Rasheed and M. Al-Khafaji.; data curation, I. Alwan.; formal analysis, N. Rasheed.; investigation, N. Rasheed.; methodology, N. Rasheed.; project administration, N. Rasheed; resources, M. Al-Khafaji.; software, N. Rasheed.; supervision, M. Al-Khafaji and I. Alwan.; validation, N. Rasheed., M. Al-Khafaji and I. Alwan.; visualization, N. Rasheed.; writing—original draft preparation, N. Rasheed.; writing—review and editing, M. Al-Khafaji. All authors have read and agreed to the published version of the manuscript.

#### Funding

This research received no external funding.

#### Data availability statement

Not applicable.

#### Conflicts of interest

The authors declare that there is no conflict of interest.

#### References

- [1] M. Biedler, *Hydropolitics of the Tigris-Euphrates River basin with implications for the European Union*, CERIS Cent. Eur. Rech. Int. Strat., 1–44, 2004.

- [2] A. A. Ali, N. A. Al-Ansari, and S. Knutsson, Morphology of Tigris river within Baghdad city, *Hydrol. Earth Syst. Sci.*, 16 (2012) 3783–3790. <https://doi.org/10.5194/hess-16-3783-2012>
- [3] M. E. Mohammad, N. Al-Ansari, I. E. Issa, and S. Knutsson, Sediment in Mosul Dam reservoir using the HEC-RAS model, *Lakes Reserv. Res. Manag.*, 21 (2016) 235–244. <https://doi.org/10.1111/lre.12142>
- [4] J. Xia, Q.-Y. Duan, Y. Luo, Z.-H. Xie, Z.-Y. Liu, and X.-G. Mo, Climate change and water resources: Case study of Eastern Monsoon Region of China, *Adv. Clim. Chang. Res.*, 8 (2017) 63–67. <https://doi.org/10.1016/j.accres.2017.03.007>
- [5] M. Gharbi, A. Soualmia, D. Dartus, and L. Masbernat, Floods effects on rivers morphological changes application to the Medjerda River in Tunisia, *J. Hydrol. Hydromech.*, 64 (2016) 56. <https://doi.org/10.1515/johh-2016-0004>
- [6] S. Hossain, M. Rahman, F. Nusrat, R. Rahman, and N. F. Anisha, Effects of climate change on river morphology in Bangladesh and a morphological assessment of Sitalakhya River, *J. River Res. Inst.*, 1 (2014) 1–13.
- [7] C. Jiang, S. Pan, and S. Chen, Recent morphological changes of the Yellow River (Huanghe) submerged delta: Causes and environmental implications, *Geomorphology*, 293 (2017) 93–107. <https://doi.org/10.1016/j.geomorph.2017.04.036>
- [8] S. Shrestha, N. Imbulana, T. Piman, S. Chonwattana, S. Ninsawat, and M. Babur, Multimodelling approach to the assessment of climate change impacts on hydrology and river morphology in the Chindwin River Basin, Myanmar, *Catena*, 188 (2020) 104464. <https://doi.org/10.1016/j.catena.2020.104464>
- [9] M. M. Altawash and H. A. Al Thamiry, Velocity Patterns inside the Proposed Makhool Dam Reservoir with Different Operation Plans, in *IOP Conf. Ser.: Earth Environ. Sci.*, 1120 (2022) 012015. <https://doi.org/10.1088/1755-1315/1120/1/012015>
- [10] N. J. Rasheed, M. S. Al-Khafaji, and I. A. Alwan, Investigation of Rivers Planform Change in a Semi-arid Region of High Vulnerability to Climate Change: A Case Study of Tigris River and Its Tributaries in Iraq, *Reg. Stud. Mar. Sci.*, 68 (2023) 103233. <https://doi.org/10.1016/j.rsma.2023.103233>
- [11] H. L. Luan, P. X. Ding, Z. B. Wang, and J. Z. Ge, Process-based morphodynamic modeling of the Yangtze Estuary at a decadal timescale: Controls on estuarine evolution and future trends, *Geomorphology*, 290 (2017) 347–364. <https://doi.org/10.1016/j.geomorph.2017.04.016>
- [12] A. H. Haghiabi and E. Zaredehdasht, Evaluation of HEC-RAS ability in erosion and sediment transport forecasting, *World Appl. Sci. J.*, 17 (2012) 1490–1497.
- [13] B. C. Singley, Sediment management and dam construction in the Dominican Republic: Case study of the Aguacate Dam, Brigham Young Univ. Hawaii, USA, Master Sci., 2013.
- [14] A. J. Schleiss, G. de Cesare, M. J. Franca, M. Pfister, Comprehensive numerical simulations of sediment transport and flushing of a Peruvian reservoir, CRC Press/Balkema, 2014. <http://dx.doi.org/10.1201/b17397-26>
- [15] A. H. Namaa, A. S. Abbasa, and J. S. Maatooqa, Hydrodynamic Model-Based Evaluation of Sediment Transport Capacity for the Makhool-Samarra Reach of Tigris River, *Eng. Technol. J.*, 40 (2022) 1573–1588. <https://doi.org/10.30684/etj.2022.135747.1282>
- [16] I. MoWRI, Ministry of Water Resources, Makhool Dam Project, Hydrological Study, 2021.
- [17] V. K. Sissakian, N. Al-Ansari, N. Adamo, J. Laue, and S. Knutsson, Geology of the Tigris River with Emphasize on the Iraqi Part, *J. Earth Sci. Geotech. Eng.*, 8 (2018) 145–166.
- [18] A. A. J. Al-Hasani, Trend analysis and abrupt change detection of streamflow variations in the lower Tigris River Basin, Iraq, *Int. J. River Basin Manag.*, 19 (2021) 523–534. <https://doi.org/10.1080/15715124.2020.1723603>
- [19] N. J. Rasheed, M. S. Al-Khafaji, and I. A. Alwan, Variations of streamflow and sediment yield in the Mosul-Makhool Basin, North of Iraq under climate change: a pre-dam construction study, *H2Open Journal*, 7 (2024) 38–60. <https://doi.org/10.2166/h2oj.2023.078>
- [20] G. J. Arcement and V. R. Schneider, Guide for selecting Manning's roughness coefficients for natural channels and flood plains, 2339. US Government Printing Office Washington, DC, 1989.
- [21] C. M. Emery, K. Larnier, M. Lique, J. Hemptinne, A. Vincent, and S. Peña Luque, Extraction of roughness parameters from remotely-sensed products for hydrology applications, *Hydrol. Earth Syst. Sci. Discuss.*, (2021) 1–40, 2021. <https://doi.org/10.5194/hess-2021-551>
- [22] K. Kuntiyawichai, W. Sri-Amporn, and C. Pruthong, Quantifying consequences of land use and rainfall changes on maximum flood peak in the lower Nam Phong river basin, *Adv. Mater. Res.*, 931 (2014) 791–796. <https://doi.org/10.4028/www.scientific.net/AMR.931-932.791>
- [23] S. Kute, S. Kakad, V. Bhoje, and A. Walunj, Flood modeling of river Godavari using HEC-RAS, *Int. J. Res. Eng. Technol.*, 3 (2014) 81–87. <http://dx.doi.org/10.15623/ijret.2014.0321017>
- [24] K. Solaimani, Flood forecasting based on geographical information system, *African J. Agric. Res.*, 4 (2009) 950–956.

- [25] V. B. Traore et al., Using of Hec-ras model for hydraulic analysis of a river with agricultural vocation: A case study of the Kayanga river basin, Senegal, *Am. J. Water Resour.*, 3 (2015) 147–154.
- [26] J. Lee and J. Ahn, Analysis of Bed Sorting Methods for One Dimensional Sediment Transport Model, *Sustainability*, 15 (2023) 2269. <https://doi.org/10.3390/su15032269>
- [27] G. W. Brunner, HEC-RAS River Analysis System: Hydraulic Reference Manual, Version 5.0, US Army Corps Eng. Eng. Cent., 547, 2016.
- [28] G. W. Brunner and S. Gibson, Sediment transport modeling in HEC RAS, in *Impacts of global climate change*, 2005, 1–12. [https://doi.org/10.1061/40792\(173\)442](https://doi.org/10.1061/40792(173)442)
- [29] S. Gibson and S. Piper, Sensitivity and applicability of bed mixing algorithms, in *World Environmental and Water Resources Congress 2007: Restoring Our Natural Habitat*, 2012, 1–12. [https://doi.org/10.1061/40927\(243\)395](https://doi.org/10.1061/40927(243)395)
- [30] S. Gibson, A. Sánchez, S. Piper, and G. Brunner, New one-dimensional sediment features in HEC-RAS 5.0 and 5.1, in *World Environmental and Water Resources Congress 2017*, 2017, 192–206. <http://dx.doi.org/10.1061/9780784480625.018>
- [31] G. Parker, Selective sorting and abrasion of river gravel. I: Theory, *J. Hydraul. Eng.*, 117 (1991) 131–147. [https://doi.org/10.1061/\(ASCE\)0733-9429\(1991\)117:2\(131\)](https://doi.org/10.1061/(ASCE)0733-9429(1991)117:2(131))